

# Flow of polycrystals in rough channels

Tanmoy Sarkar,<sup>1</sup> Pinaki Chaudhuri,<sup>2</sup> and Anirban Sain<sup>1,\*</sup>

<sup>1</sup>*Department of Physics, Indian Institute of Technology, Bombay, Powai, Mumbai-400 076, India.*

<sup>2</sup>*Institute of Mathematical Sciences, CIT Campus, Taramani, Chennai 600113, India*

(Dated: May 30, 2021)

Polycrystals are partially ordered solids where crystalline order extends over mesoscopic length scales, namely, the grain size. We study the Poiseuille flow of such materials in a rough channel, and observe that the response can be very different, compared to amorphous materials. In general, similar to yield stress fluids, three distinct dynamical states, namely, flowing, stick-slip and jammed can be observed, depending on the channel width and applied body force (e.g., gravity). Importantly, the interplay between the finite system size (the channel width), and the inherent ordering scale (the grain size) leads to new type of spatiotemporal heterogeneity. In relatively wide channels, although the average flow profile remains simple plug like, at the underlying granular level, there is vigorous grain remodelling activity resulting from the velocity heterogeneity among the grains. As the channel width approaches typical grain size, the flowing polycrystalline state surprisingly breaks up into a spatially heterogeneous mixture of flowing liquid like patches and chunks of nearly static grains. Despite these static grains, the average velocity still shows a parabolic profile, dominated by the moving liquid like patches. However, the solid-liquid front moves at nearly constant speed in the opposite direction of the external drive.

## I. INTRODUCTION

Most solids in nature are found in either polycrystalline or amorphous forms. Polycrystals have mesoscopically large ordered regions, the grains, which are separated by atomistically narrow disordered grain boundaries, across which the grain orientation changes abruptly. On the contrary, in amorphous materials, there is no spatial order in the arrangement of atoms. So, in terms of the degree of spatial heterogeneity, polycrystals fall in between single crystal and amorphous material [1]. How does the intrinsic ordering scale, the grain size, makes polycrystals different in terms of dynamic response? It has been shown that polycrystals, under shear, share some of the flow properties (vortices, saddles etc.) of amorphous material [2], yet retaining unique features like grain rotation, dislocation creep etc. Driven flow of such materials through a static channel (under gravity or pressure gradient, for example) introduces an additional length scale, namely, the boundary layer thickness, as the channel walls try to resist the motion where as the driving force tries to maintain the motion. In such a situation does a polycrystal break down into amorphous state or can it maintain a coexistence of both amorphous and polycrystalline states? We probe this question, using numerical simulations.

Compared to polycrystals, flow properties of amorphous materials have been much more widely studied. A thin layer of concentrated emulsion moving through a rough channel of adjustable width [3, 4] shows finite size effect driven transition from plug like flow profile to parabolic flow profile as the channel width is reduced. Similar plug like flow is also reported in colloidal gel at intermediate density [5, 6], concentrated colloidal suspensions [7], ultra-soft particles [8]. Interestingly, in narrow rough channels a backward moving density wave has been reported in flows of dense colloidal suspension [9–12] and granular particles [13]. Similar waves have been reported for traffic flows in highways [14]. Such density fluctuations takes the form of an S-shaped wave and a clump when granular material [15] flows down rapidly through a vertical channel under gravity. Denser granular flow [16] phase separates into fluid like low density region near the boundary and a denser solid plug-like flow structure around the centre of the channel.

In this letter, using molecular dynamics simulations, we report a study of the flow response of a 2D model soft polycrystalline system, confined in a rough channel and subjected to a constant body force (e.g., gravity). In the case of a wide channel, i.e. when channel width  $w \gg d$ , the particulate diameter, we get a plug like flow profile with a significant boundary layer, even in the presence of grains and velocity heterogeneity in grain velocities. This is qualitatively different from that in granular media. On the other hand, for narrow channels when ( $w \approx 10d$ ), a significant fraction of the polycrystal melts and interestingly, the fluid-solid front moves at a constant speed in the opposite direction of the main flow; similar phenomena has been reported in granular media.

---

\* asain@phy.iitb.ac.in

## II. MODEL

For our study, we considered a weakly bidisperse, two-dimensional Lennard-Jones (LJ) system with total number of particles  $N = 12118$ . By choosing the fraction of large particle as 1% and the size ratio of 1.4, we generate polycrystalline states [17]. We worked at volume fraction  $\phi = 1$  and temperature  $T = 0.2$ . We choose weakly bidisperse system because mono-disperse polycrystals with LJ potential is unstable under external drive and tend to form single crystal after long time. However, the weakly bidisperse system can sustain a polycrystalline non-equilibrium steady state, under shear [18, 19]. The Poiseuille flow is set up in a rectangular 2D geometry with two confining walls perpendicular to the y-axis and periodic boundary conditions along x axis. We implemented a thermostat, by dividing the system into thin slabs parallel to the external force and rescaling the temperature regularly after every few iterations. We fill the simulation box with a preformed polycrystalline sample, using the above parameter. To generate the Poiseuille flow, only the particles within a slab, of width  $w$ , parallel to  $\hat{x}$  axis, centred around the middle of the box, were subjected to an additional constant external force  $F_{ext}\hat{x}$ . The static particles above and below the slab, which interact via the LJ potential with the flowing particles, serve as the rough channel walls. The width  $w$  of the slab was systematically varied to study the flow for different confinements.

## III. RESULTS

Our MD simulation shows that at a coarse grained level the flow behaviour of the confined polycrystal resembles that of amorphous solids [3, 4, 20]. However, the underlying grain dynamics in polycrystals gives rise to some distinct features which is not captured by the average flow profile, and is the focus of this article. Due to friction at the rough channel walls, the polycrystals resists motion till  $F_{ext}$  increases beyond a threshold. In Fig.1 we show an approximate phase diagram, in terms of the width  $w$  and the wall stress, defined by  $\sigma_w = \rho F_{ext}w/2$  [21]. Interestingly, as the system transits from a stuck (jammed) to a flowing state, with the increase in  $F_{ext}$ , an intermediate state, with stick-slip motion, is observed. The width of the stick-slip region along the vertical axis decrease at large width.

Under nonequilibrium steady state conditions, for large channel width  $w$ , the flow profile of the soft polycrystal exhibits fluid like behaviour. At large width  $w$ , the spatially averaged flow profile,  $v_x(y)$ , is plug like (see inset of Fig.1) in the bulk and has high, but nearly constant, velocity gradient near the walls, resembling boundary layer. In contrast, for narrow channels, the averaged flow profile  $v_x(y)$  is parabolic (inset of Fig.1) as in the case of low Reynolds number (viscous) pipe flow. We will discuss this, in more details, later.

For the plug flow regime, while amorphous structure prevails in the boundary layer, polycrystalline grain structure is maintained in the bulk, see top panel of Fig.2. However, the grain structure constantly remodels via grain break-up and coalescence [19]. Fig.2 shows the changing grain structure of the flowing polycrystal as time evolves. We use a "disorder variable", following Ref.[17], which captures the local arrangement of the particles and can clearly demarcate the grain boundaries. In the top panel of Fig.2, the plots (a),(b) show growth of grains in time. The bigger grains eventually break up (not shown here) into smaller ones. Despite this dynamic cycle of grain growth and breakage continuing in the bulk, the average flow profile remains plug like. Note that even in dense, soft, glassy material [3] such plug to parabolic flow transition, with decreasing channel width, was reported but the internal structure and dynamics in the plug region, reported here, is unique to polycrystals.

The existence of plug like flow despite the continuous grain remodelling requires an explanation, which is illustrated via the bottom-left panel of Fig.2. In the left panel, the sub-plot (a) shows an example snapshot of the particle velocities in half of the simulation box. Here, we note two interesting features, first, particle velocities are inhomogeneous, and second, a distinct grain structure is manifested. Two enclosed boxes in the bulk of subpanel(a) are zoomed in subpanels (b) and (c), where the grain boundaries are shown by broken lines. Subpanel (b) shows a moving triple junction of grains, where all the particles have almost the same forward velocity, although the crystal glide planes are different in the three grains. This feature is consistent with the plug like flow profile in the bulk. On the otherhand, there is a nearly constant velocity gradient in the boundary layer. One can imagine that the whole bulk region, at the centre, moves at a constant speed like a rigid block, cushioned by liquid layers separating it from the walls. Thus, each of the boundary liquid layers is confined between the moving block and the wall, and therefore responds as a Couette flow with constant velocity gradient. However, if this was the complete picture, then the grains in the bulk would not grow or break. In the subpanel (c), we show only the velocity components of the particle, transverse to the flow direction (with enhanced magnification than in (b)). Indeed, there are correlated particle motions in the transverse direction, i.e. non-affine displacements, which will lead to slow shearing of the grains, and eventual breakage/coalescence. However, this overall scenario, breaks down in a narrow channel which we will discuss later.

To quantify this dynamic heterogeneity, we further computed the time evolution of the dislocation population  $N_d$ , a marker that is distinct for polycrystals, unlike amorphous systems. A dislocation in this 2D system is defined by a pair of neighboring particles with coordination number five and seven. In particle configurations shown in the top

panel of Fig.2 (a),(b), such pairs are found at the grain boundaries and near the confining walls. Inset of Fig.2(c) shows temporal fluctuation of  $N_d$  and the main figure shows the corresponding power spectrum, which scales as  $\frac{1}{\omega^2}$  over almost one decade of frequency. Interestingly, the same scaling behaviour was reported for sheared polycrystals in Ref[22].

Distribution of particle displacements  $P(u)$ , where  $u$  is the magnitude of the 2D displacement, is an useful marker for spatio-temporal heterogeneity in amorphous material [2, 23]. In the right-bottom panel of Fig.2, we show this distribution for various time intervals  $t$ . They all collapse onto a master curve when  $P(u)$  and  $u$  are appropriately scaled (see Fig.2 (bottom-right)). This implies a stationary pattern of displacements originating from different regions of the channel and the scaling can be understood from the average velocity profile. The distribution (see Fig.2 (bottom-right)) curves have three parts. The dominant peak is populated by the movements of particles from the bulk region that exhibits plug flow. The nearly horizontal part of the distribution can be rationalised as follows : the mean velocity profile  $v(y) \approx \frac{y}{t}$  is approximately linear in  $y$ , the distance from the walls. In the distribution (histogram) the particles with displacements between  $u$  and  $u + du$  come from the strip of width  $dy$  and length  $L$ , thus  $P(u)du \propto dy.L$ . The linear profile near the wall gives  $dy \propto du/t$ . Using this we get  $P(u)t = \text{constant}$  i.e,  $P(u)t$  is independent of  $u$ . Furthermore, to characterize the velocity fluctuation we define a non-dimensional velocity  $\Delta v_x = \frac{v_x - \langle v_x(y) \rangle}{v_{rms}}$  where  $v_x$  is the instantaneous velocity along  $\hat{x}$ ,  $\langle v_x(y) \rangle$  is the average velocity and  $v_{rms}$  is the rms velocity. The non-dimensional velocity fluctuation shows a non-Gaussian distribution that deviates at the tails, see inset of Fig.2 (bottom-right). Interestingly, similar non-Gaussian distribution has been reported in dense granular flows [24–26].

Qualitatively new flow behaviour emerges when the channel is narrow ( $w \approx 10d$ ), and the rheological response is probed in the vicinity of the yield threshold ( $\sigma_w = 6.4$ ). The moving polycrystal disintegrates into chunks of crystallites and fluid like patches, along the length of the channel; see Fig.3. In the upper four panels, we show snapshots of particle positions, with time increasing upwards, as indicated, using the disorder variable representation, which clearly differentiates the crystalline and fluid zones. We also observe that the density in the fluid zone is also relatively less. In the bottom most panel (which is a replica of the panel just above it), we superpose the particle velocities, in few narrow vertical strips. It is evident that the particles in the fluid zones move fast while the crystalline zones are nearly static with small random velocities. Yet, the flow profile  $v_x(y)$ , averaged along the flow direction ( $\hat{x}$ ), is parabolic (see inset of Fig.1), which is mainly contributed by the liquid like regions, where the profile is strongly parabolic. Thus, from the average flow profile, it is not possible to guess about the underlying density stratification. Although the solid-liquid interfaces are not sharp in Fig.3, it appears that the interface is moving left, in the opposite direction of the main flow. Before probing this in details, we note that density waves were reported in gravity-driven granular flows and traffic flows [14, 15]. Also, in experiments with driven, dense colloidal suspensions, backward moving density waves were reported [9, 27] and modelled [10]. However, note here, that in our case, we have no explicit solvent, as was invoked in discussing such observations in experiments [9] or for modeling [10].

To capture the motion of the diffuse liquid-solid interface, we constructed an effective coarse grained, 1-D density field by integrating the particle number density along the  $y$  direction. The central panel of Fig.3 shows density snapshots at successive time intervals. The liquid patch (the low density dark region) can be seen moving to the left at nearly constant speed (as the kymograph is linear). To confirm this effect, in the bottom panel of Fig3 we recorded the average particle velocity  $\langle v_x(t) \rangle$  in a fixed area element, at the centre of the channel, as a function of time. Almost regular temporal oscillations can be seen. The corresponding Fourier transform of  $|\langle v_x(\omega) \rangle|$  shows a dominant peak and a weak first harmonic, see inset-b. In inset-a, we present the velocity distribution  $P(v_x)$  of all the particles in the channel. The distribution is asymmetric and gets higher weightage from the positive side, implying that the average velocity is rightward. We checked that the positive tail at high  $v_x$  is contributed by the fast moving liquid particles and the maxima at small positive  $v_x$  comes from the crystalline regions.

The low density liquid patch moves backward essentially by treadmilling. Consider a liquid patch in between two solid blocks. The exposed layer from the left block melts into liquid due to  $F_{ext}$  and thermal forces, and the "atoms" move right due to  $F_{ext}$ . This way the left front of the liquid moves one atomic spacing to the left. At its right front, right moving "atoms" from the liquid, driven by  $F_{ext}$  add a new layer to the solid block on the right. So the right front of the liquid moves left by one unit. The melting occurs as  $F_{ext}$  overcomes cohesion force of the LJ solid and the melting rate is expected to be constant provided the number densities in both the solid and the liquid attains steady values. Note that in this mechanism a given particle periodically changes its membership between the solid and liquid regions, and moves slow and fast accordingly.

#### IV. SUMMARY AND DISCUSSIONS

In summary, we showed how grain size, the additional length scale in polycrystals, makes its flow properties in rough channels different from that in granular media. At large channel width, the dynamic heterogeneity in terms of the grain dynamics does not have any parallel in granular media, but for narrow channels the transverse density

stratification and the backward moving low density wave have analogs in granular case, although there grains are absent. The density stratification parallel to the flow, into boundary layer and bulk that occurs at large channel width, drastically switches to transverse stratification into solid and liquid zones, when channel width is reduced. This transition is a finite size driven effect when the channel width becomes comparable to typical grain size in the bulk. Interestingly the switching does not require any change in overall density. We hope that all these observations can be realised in colloidal polycrystals in real experiments.

- 
- [1] L. Berthier, *Physics* **4**, 42 (2011).
  - [2] S. Biswas, M. Grant, I. Samajdar, A. Haldar, and A. Sain, *Scientific reports* **3** (2013).
  - [3] J. Goyon, A. Colin, G. Ovarlez, A. Ajdari, and L. Bocquet, *Nature* **454**, 84 (2008).
  - [4] V. Mansard, A. Colin, P. Chaudhuri, and L. Bocquet, *Soft matter* **9**, 7489 (2013).
  - [5] M. T. Roberts, A. Mohraz, K. T. Christensen, and J. A. Lewis, *Langmuir* **23**, 8726 (2007).
  - [6] J. C. Conrad and J. A. Lewis, *Langmuir* **24**, 7628 (2008).
  - [7] L. Isa, R. Besseling, and W. C. Poon, *Physical Review Letters* **98**, 198305 (2007).
  - [8] A. Nikoubashman, G. Kahl, and C. N. Likos, *Soft Matter* **8**, 4121 (2012).
  - [9] L. Isa, R. Besseling, A. N. Morozov, and W. C. K. Poon, *Phys. Rev. Lett.* **102**, 058302 (2009).
  - [10] P. Kanehl and H. Stark, *Phys. Rev. Lett.* **119**, 018002 (2017).
  - [11] M. Haw, *Physical review letters* **92**, 185506 (2004).
  - [12] A. I. Campbell and M. D. Haw, *Soft Matter* **6**, 4688 (2010).
  - [13] S. Horikawa, T. Isoda, T. Nakayama, A. Nakahara, and M. Matsushita, *Physica A: Statistical Mechanics and its Applications* **233**, 699 (1996).
  - [14] B. S. Kerner and P. Konh user, *Physical Review E* **48**, R2335 (1993).
  - [15] E. D. Liss, S. L. Conway, and B. J. Glasser, *Physics of Fluids* **14**, 3309 (2002).
  - [16] E. Khain, *Mathematical Modelling of Natural Phenomena* **6**, 77 (2011).
  - [17] H. Shiba and A. Onuki, *Physical Review E* **81**, 051501 (2010).
  - [18] T. Hamanaka and A. Onuki, *Physical Review E* **74**, 011506 (2006).
  - [19] T. Sarkar, S. Biswas, P. Chaudhuri, and A. Sain, *Physical Review Materials* **1**, 070601 (2017).
  - [20] P. Chaudhuri and J. Horbach, *Physical Review E* **90**, 040301 (2014).
  - [21] P. Chaudhuri, V. Mansard, A. Colin, and L. Bocquet, *Physical review letters* **109**, 036001 (2012).
  - [22] J. M. Tarp, L. Angheluta, J. Mathiesen, and N. Goldenfeld, *Physical review letters* **113**, 265503 (2014).
  - [23] P. K. Jana, M. J. Alava, and S. Zapperi, *Scientific Reports* **7**, 45550 (2017).
  - [24] S. Moka and P. R. Nott, *Physical review letters* **95**, 068003 (2005).
  - [25] A. V. Orpe and A. Kudrolli, *Physical review letters* **98**, 238001 (2007).
  - [26] K. Ananda, S. Moka, and P. R. Nott, *Journal of Fluid Mechanics* **610**, 69 (2008).
  - [27] S. Horikawa, A. Nakahara, T. Nakayama, and M. Matsushita, *Journal of the Physical Society of Japan* **64**, 1870 (1995).

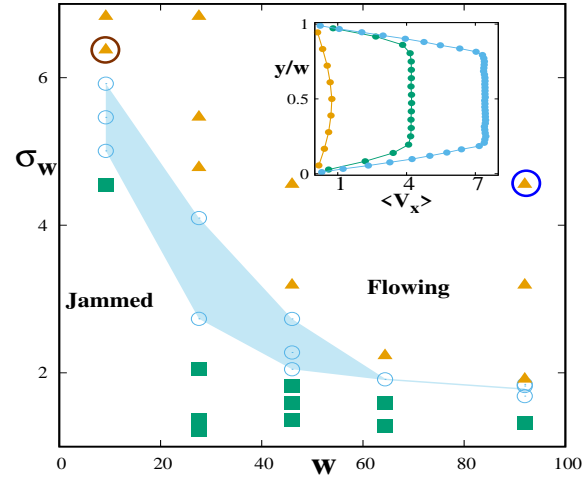


FIG. 1. Phase plot as a function of channel width  $w$  and wall stress  $\sigma_w$ . Three different dynamical states are identified: flowing (triangles), stick-slip (circles) and jammed (squares). The shaded region represent the stick-slip states. The inset shows the averaged velocity profile  $v_x(y)$  plotted as a function of  $y$  (scaled by  $w$ ). In the three plots, from left to right, the flow profile changes from parabolic to plug as the channel is widened. The corresponding parameters are  $(w, \sigma_w) = (9.2, 6.4)$ ,  $(27.6, 5.5)$  and  $(46, 4.6)$ .

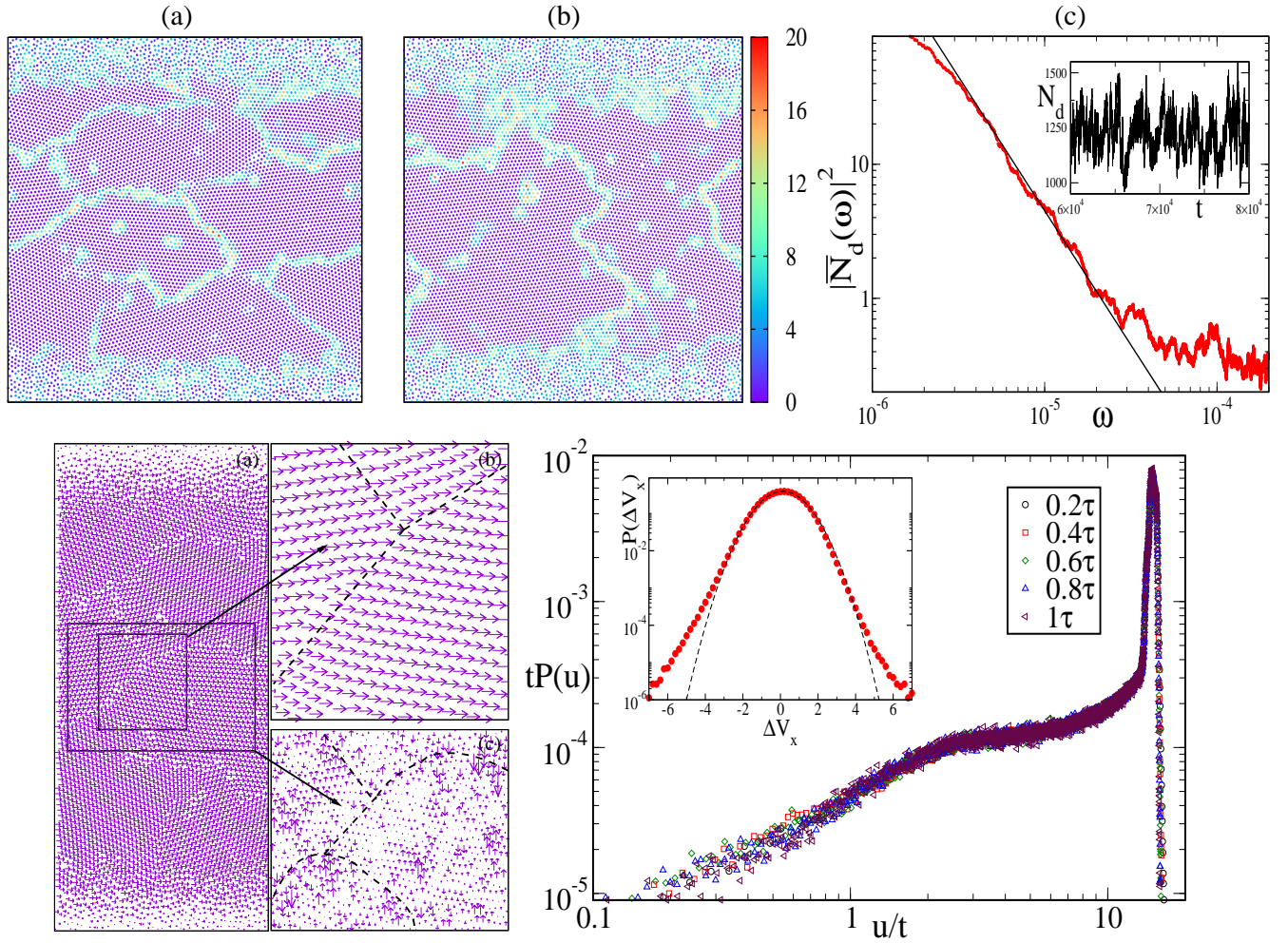


FIG. 2. **(Top)** Flow in a wide channel ( $w = 92, \sigma_w = 4.6$ ), shows visible grains. Colour bar shows value of disorder variable [17]. (a)  $\rightarrow$  (b) shows growth of grains in time. In the steady state growth is followed by grain break up. (c) shows corresponding power spectrum of dislocation number ( $N_d$ ) fluctuation. The black line shows a  $\frac{1}{\omega^2}$  fit to the spectrum. Inset of (c) shows fluctuation of  $N_d$  with time. **(Bottom) [Left]**. (a) Heterogeneous velocity pattern in a wide channel (half the channel is shown). A triple grain junction in (a) is zoomed in (b) and (c). While (b) shows the full velocity vector for each particle, (c) shows only the  $v_y$  component, in order to highlight the velocity heterogeneity among grains. **[Right]**. Displacement distribution collected at different time intervals  $t$ , in wide channel ( $w = 91.99, \sigma_w = 4.55$ ). The distributions collapsed when both the axes are appropriately scaled with the interval  $t$ . Here, different symbols represent different time intervals  $t$ , specified in the legend box. The inset shows distribution of nongaussian velocity fluctuation along the flow. The dashed line is a gaussian fit.

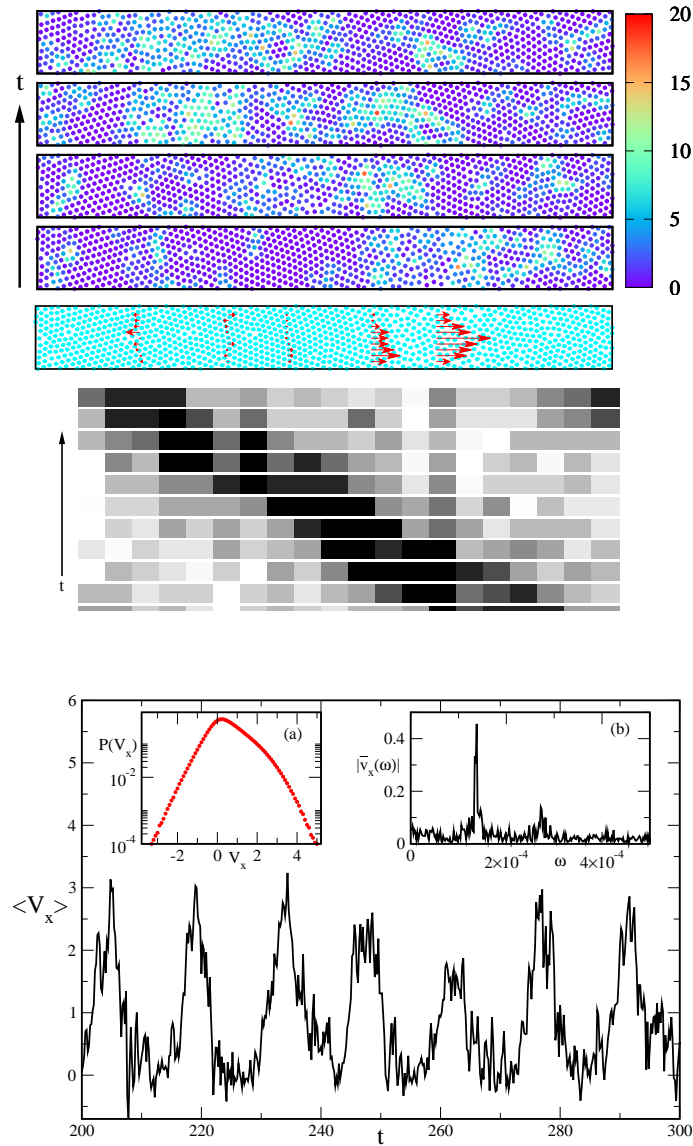


FIG. 3. Fluidization of a flowing polycrystal in narrow channel ( $w = 9.2, \sigma_w = 6.4$ ). **(Top)** The first four panels show a moving patch of fluid, with time increasing upwards. Colour bar shows value of the disorder variable. The bottom most panel shows heterogeneous velocity map of the earliest snapshot, on five vertical strips. **(Center)** The corresponding density map, to show that the fluid front moves in the opposite direction of the applied body force in a narrow channel; darker the colour, lower is the density. **(Bottom)** Average particle velocity in a small area element at the center of the narrow channel along the direction of the drive. Nearly periodic oscillations imply that the liquid patch moves at a relatively high and constant speed across the channel. Inset (a) shows velocity distribution of all particles, with its maximum at a non-zero positive value, mainly contributed by the particles from the slow moving crystalline regions. Inset (b) shows presence of a peak and harmonics in the corresponding Fourier spectrum.